

## Article

# Seasonal Variability and Hydrological Patterns Influence the Long-Term Trends of Nutrient Loads in the River Po

Edoardo Cavallini <sup>1</sup>, Pierluigi Viaroli <sup>1</sup>, Mariachiara Naldi <sup>1</sup>, Mattia Saccò <sup>1,2</sup>, Alessandro Scibona <sup>3</sup>, Elena Barbieri <sup>3</sup>, Silvia Franceschini <sup>4</sup> and Daniele Nizzoli <sup>1,\*</sup>

- <sup>1</sup> Department of Chemistry, Life Sciences and Environmental Sustainability, University of Parma, Parco Area delle Scienze 11/A, 43124 Parma, Italy; edoardo.cavallini@unipr.it (E.C.); pierluigi.viaroli@unipr.it (P.V.); mariachiara.naldi@unipr.it (M.N.); mattia.sacco@curtin.edu.au (M.S.)
- <sup>2</sup> Subterranean Research and Groundwater Ecology (SuRGE) Group, Trace and Environmental DNA (TrEnD) Lab, School of Molecular and Life Sciences, Curtin University, Perth, WA 6102, Australia
- <sup>3</sup> Po River Basin District Authority, Technical Unit 2—Water Planning and Management, Strada Garibaldi n. 75, 43121 Parma, Italy; alessandro.scibona@adbpo.it (A.S.); elena.barbieri@adbpo.it (E.B.)
- <sup>4</sup> Emilia-Romagna Regional Agency for Environmental Protection and Energy, West Environmental Prevention Area, Reggio Emilia Headquarters, Via Amendola 2, 42122 Reggio Emilia, Italy; sfranceschini@arpae.it
- \* Correspondence: daniele.nizzoli@unipr.it

**Abstract:** This study investigates the long-term trends (1992–2022) of nitrogen and phosphorus loadings exported by the River Po to the Adriatic Sea, to better analyse how changes in hydrology are affecting the timing and magnitude of river nutrient loads. We used 30 years of monitoring data in order to (a) identify the main temporal patterns and their interactions at a decadal, annual and seasonal scale, (b) estimate precipitation effects on load formation and evaluate whether and to which extent the hydrological regime affects nutrient export across the years and (c) analyse the nutrient export regime at a monthly scale and the main transport dynamic of N and P chemical species (hydrological vs. biogeochemical control). The long-term analysis shows a general decrease of both P and N loadings, but the trends are different between the elements and their chemical species, as well as undergoing different seasonal variations. We found a statistically significant relationships between precipitation and loads, which demonstrates that precipitation patterns drive the exported load at the intra- and interannual time scales considered in this study. Precipitation-induced load trends trigger seasonal changes in nutrient deliveries to the sea, peaking in spring and autumn. The nitrogen decrease is mainly concentrated in the summer dry period, while total phosphorus diminishes mainly in spring and autumn. This mismatch of N and P results in variable molar N:P ratios within the year. The effects of extreme drought and flood events, along with the progressive decrease in the snowmelt contribution to water fluxes, are expected to exacerbate the variability in the N and P loadings, which in turn is expected to perturbate the biodiversity, food webs and trophic state of the Northern Adriatic Sea.

**Keywords:** nitrogen; phosphorus; loading; long-term trends; seasonality; precipitation; discharge



**Citation:** Cavallini, E.; Viaroli, P.; Naldi, M.; Saccò, M.; Scibona, A.; Barbieri, E.; Franceschini, S.; Nizzoli, D. Seasonal Variability and Hydrological Patterns Influence the Long-Term Trends of Nutrient Loads in the River Po. *Water* **2024**, *16*, 2628. <https://doi.org/10.3390/w16182628>

Academic Editor: Achim A. Beylich

Received: 5 August 2024

Revised: 10 September 2024

Accepted: 12 September 2024

Published: 16 September 2024



**Copyright:** © 2024 by the authors. Licensee MDPI, Basel, Switzerland. This article is an open access article distributed under the terms and conditions of the Creative Commons Attribution (CC BY) license (<https://creativecommons.org/licenses/by/4.0/>).

## 1. Introduction

Widespread alterations in nutrient cycling are occurring in river basins at a global level due to the increased intensity of land use, i.e., agriculture, livestock and urbanisation, as well as hydro-morphological modifications and climate change [1–4]. These pressures result in excessive nitrogen (N) and phosphorus (P) delivery to both inland and marine coastal waters, which triggers degenerative eutrophication processes and unprecedented nitrate pollution, especially in lentic aquatic ecosystems [5–8]. The detrimental impact of nitrogen and phosphorus pollution has led to significant efforts to regulate nutrient loading, but the outcomes of these efforts have been contrasting, due to the complex and often cumulative nature of the factors involved [7].

The relationships between anthropogenic N/P loadings and eutrophication processes are commonly assessed, assuming the inter-dependence between both elements in running waters and their anthropic input derived from climate and hydrological patterns [5,7,9–12]. However, the environmental pathways and fate of N and P are not simply dependent on their sources, as they are also affected by several other factors, including the chemical speciation of N (e.g., the ammonium (N-NH<sub>4</sub><sup>+</sup>) to nitrate (N-NO<sub>3</sub><sup>-</sup>) ratio), the biological availability of P compounds, the river metabolism and the interactions between the river and its floodplain, including the interchange with lateral wetlands [13–17].

Besides anthropogenic sources, N or P availability and their chemical speciation are often regulated by so-called “flood pulses” [18]. Many rivers and streams are impacted by an altered flow and water temperature, especially in the temperate regions, where the frequency of flood events and prolonged drought periods is dramatically increasing due to climate change [19–22]. The resulting alternation of such different conditions can deeply modify the mobility and availability of N and P forms, which depend on, e.g., oxygen availability, sedimentary microbial metabolism, sediment sorption properties and redox-sensitive metals, as well as the precipitation effect on soil erosion [23–27]. The fluctuation in water level induces the alternation of dry phases, causing the exposure to air of soils and riverbeds (the oxic-oxidative phase), followed by flooding (the anoxic-reducing phase), which support nitrification and denitrification processes, respectively [28,29]. Concurrently, inorganic P forms are adsorbed and retained by soil particles in the dry phase, whilst they are released/desorbed and transported by the surface runoff in the wet phase [27,30,31]. In the river basins of temperate zones, these processes are expected to undergo nearly regular seasonal patterns depending on a series of factors: precipitation, heat budget/temperature, evapotranspiration, water abstraction for irrigation and river metabolism. Collectively, these components affect the long-term trends of nutrient loadings [12,32,33]. Over the last decades, climate changes have deeply modified the seasonality of both the river discharge and nutrient loadings, due to the occurrence of severe and prolonged droughts, followed by heavy short-term rainfalls or exceptional snowmelt and flash floods [34–36]. Under these conditions, river runoff is expected to deliver high amounts of soluble N-NO<sub>3</sub><sup>-</sup>, along with particulate P [37–39]. The chemical speciation of N, namely the N-NH<sub>4</sub><sup>+</sup> to N-NO<sub>3</sub><sup>-</sup> ratio, influences N reactivity and bioavailability, and the inherent risk of the N-NO<sub>3</sub><sup>-</sup> pollution of both surface water lenses and groundwater. Therefore, N and P may differentially impact downstream ecosystems: N-NO<sub>3</sub><sup>-</sup> is usually promptly reactive [40,41], whereas soluble reactive phosphorus (SRP) is closely associated with soil/sediment particles, which are usually much less reactive and bioavailable than N-NO<sub>3</sub><sup>-</sup> [31].

As a result, land use and morphological modifications, along with precipitation and global warming, may modify not only the annual nutrient loading delivery to coastal zones, but also its stoichiometry and timing/seasonality [42–44]. Variations in the precipitation regime, coupled with a higher frequency of extreme drought and rainfall/storm events, along with snowfall and snowmelt dynamics, may further coincide to modify nutrient transport and its fate in the catchment [45–47]. Importantly, the onset of hydrological intermittence is challenging our capacity to discriminate which factors, and at which temporal scale, have the potential to influence the eutrophication of the receiving waterbodies [24,48]. Additionally, much of the research focuses on the fate of N species compared to P species. Importantly, N and P may respond differently to climate change, resulting in variations in N:P ratios with different effects on the quality of downstream ecosystems [49,50]. Understanding the role of climate patterns and human activity in driving nutrient loads is therefore pivotal for distinguishing the temporal trajectories of the various nutrient regimes and their drivers [7]. In this context, long-term monitoring plays a critical role in verifying the effect of multiple factors and their interaction on a seasonal level. Long-term analyses allow for the inclusion of extreme periods or events that are rare by definition, despite their frequency being one of the main controlling factors of nutrient export [51].

This study aims to analyse decadal, annual and seasonal trends of N and P loads to better elucidate how changes in hydrology affect the timing and magnitude of riverine

nutrient loads. We focused our analysis on the River Po basin in Northern Italy, which is facing an increasing impact of severe drought events [36,52], as well as the progressive volume loss of alpine glaciers due to climate change [34,53]. Here, rivers and streams are currently undergoing hydrological intermittence due not only to global changes, but also to increasing local anthropogenic pressures on aquatic ecosystems [51,54]. Nutrient loadings delivered to the Adriatic Sea have been studied since the late 1960s [55]. Detailed studies were performed in the early 2000s, aiming at relating anthropogenic sources and hydrological variability to riverine loadings [12,56,57] and studying natural processes of N removal [58]. However, while most studies investigated nutrient interannual variations, they did not focus on the influence of hydrology on seasonal changes and how this can contribute to long-term trends. To cover this gap in research, in this study we aim to (i) identify the main temporal patterns at a decadal, annual and seasonal scale to unveil the interplay between these different time intervals, (ii) assess precipitation effects on load formation and evaluate whether changes in the hydrological regime are affecting the export of nutrients across the years and (iii) analyse the nutrient export patterns at a monthly scale, with a specific focus on the main transport dynamic of N and P chemical species (hydrological vs. biogeochemical control).

Our overarching hypothesis is that changes in hydrological characteristics can influence decadal changes in nutrient export by affecting the intra-annual load distribution, but the effect depends on nutrient-specific transport pathways. To test this hypothesis, we analysed N and P loads and their ecological stoichiometry over three decades (1992–2022). We also analysed interannual changes in precipitation and water discharge and their relationships with nutrient concentrations and loadings. This approach (i.e., c-Q metrics) is applied to capture the integrative influence of climate and hydrology on nutrient transport, and it has already provided crucial information on the processes controlling the mobilisation and delivery of chemical elements into streams (i.e., export regimes), as well as biogeochemical transformations in river networks [50,59–61].

## 2. Materials and Methods

### 2.1. Study Area

The River Po is 652 km long and is the second largest river in the Mediterranean Sea in terms of water discharge (Q) after the Rhône, while is the first considering total phosphorus and nitrogen exported loads [56,62]. The River Po basin is 74,000 km<sup>2</sup>, of which 71,000 km<sup>2</sup> (~46,000 km<sup>2</sup> as lowland) is in Italy (Figure 1); its geographical area covers almost one-fourth the total land surface of Italy, and ~40% of the Italian GDP is generated in the Po region [63]. The basin is largely anthropised, with 49% of the area covered by arable land (42%) and artificial surfaces (7%), whereas the remaining is composed of forest and seminatural areas (49%) (Figure S1) (CLC 2018, <https://doi.org/10.2909/71c95a07-e296-44fc-b22b-415f42acfd0>, accessed on 28 August 2024).

The River Po basin is characterised by a heterogeneous orography, with an altitude varying from 0 to 4792 m a.s.l (mean = 498 m a.s.l) (Figure S2) (<https://ec.europa.eu/eurostat/web/gisco>, accessed on 28 August 2024). The Alps (from the west to the north side) and Apennines (south side) encircle the Po plain, strongly affecting the climate. The mean air temperature ranges from 5 °C in the alpine zone, to 10 °C in the Prealpine and Apennine areas, reaching 15 °C in the Po plain. Minimum values occur in January and maximum in July. The yearly mean precipitation is 1080 mm; however, it is heterogeneously distributed. The Central Alps and Apennines show highest precipitation values (>1200 mm), while in some areas of the Po plain precipitation is below 700 mm [64].

Overall, the southern side of the basin is affected by water scarcity, and streams and rivers have extremely variable flow regimes. Contrarily, the northern side of the basin has a great number of reservoirs and high-altitude small lakes, as well as four large deep subalpine lakes fed by alpine glaciers (Maggiore, Como, Iseo, Garda). These four lakes account for ~70% of the water volume of surface freshwater in Italy and feed the main tributaries of the River Po, which make up about 50% of its total water discharge [64,65].

Finally, agriculture interferes heavily with the hydrological cycle, with  $\sim 22 \text{ km}^3 \text{ y}^{-1}$  of water being used for irrigation. Remarkably, this volume represents approximately 50% of the average annual discharge of the River Po and is almost equivalent to the summer water flux in the basin [66].

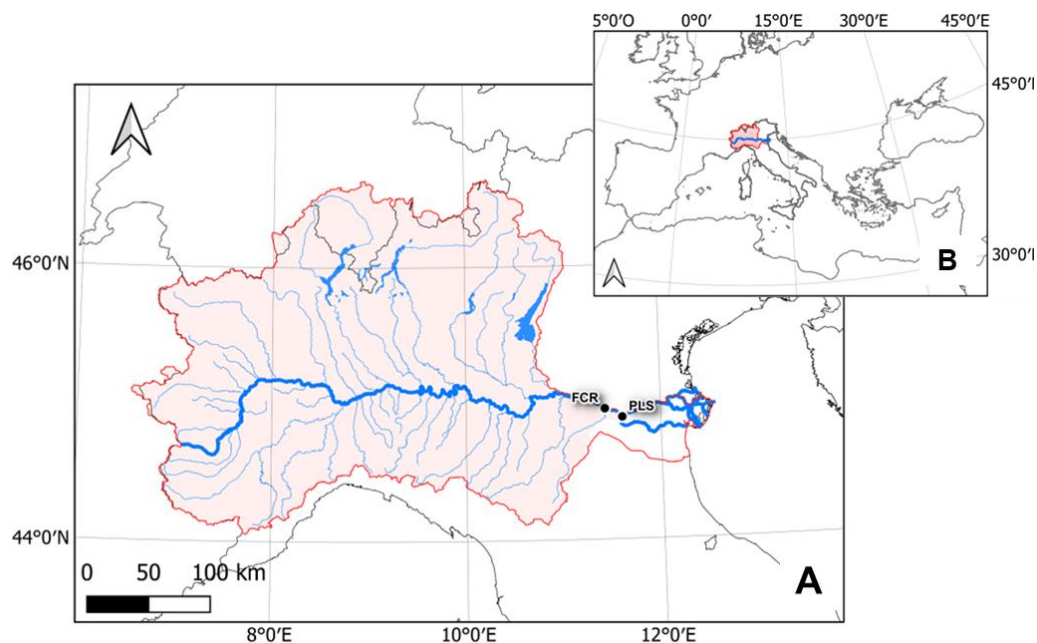


**Figure 1.** The main map (A) shows the River Po basin with the River Po, its main tributaries and the subalpine lakes. The red solid line delimits the River Po basin, while the shaded region specifically identifies the part of the basin covered by the Pontelagosuro (PLS, N  $44^{\circ}53'17''$ –E  $11^{\circ}36'29''$ ) and Ficarolo (FCR, N  $44^{\circ}56'42''$ –E  $11^{\circ}25'31''$ ) closing stations; the small map (B) places the River Po basin within the Mediterranean area.

## 2.2. Datasets and Temporal Resolution

The closing station of the River Po basin is historically positioned at Pontelagosuro village (PLS) (Figure 1). The monitoring of water quality and quantity are routinely conducted by the Emilia-Romagna Regional Agency for Environmental Protection (ARPAE).

Nutrient concentration data from 1992 to 2009 were directly provided by ARPAE, whereas data from 2010 to 2022 are freely available for download from their website ([https://dati.arpae.it/dataset?q=rete-regionale-per-la-qualita&sort=score+desc,+metadata\\_modified+desc](https://dati.arpae.it/dataset?q=rete-regionale-per-la-qualita&sort=score+desc,+metadata_modified+desc)) and were accessed on 2 October 2023. The dataset for this study includes fortnightly samplings from 1992 to 2000, and monthly samplings from 2001 to 2022. Phosphorus (TP, SRP) and inorganic nitrogen (N-NH<sub>4</sub><sup>+</sup>, N-NO<sub>3</sub><sup>-</sup>) data were available for the entire 30-year period, 1992–2022. The sample collection and analytical determinations were performed according to the standard methods and analytical protocols indicated by IRSA-CNR [67].

Daily water discharge data are also freely available from the ARPAE online repository, DEXT3R (<https://simc.arpae.it/dext3r/>, accessed on 2 October 2023), and were downloaded for the period 1992–2022. Missing data for time intervals shorter than a few days were replaced by linear interpolation, whereas missing data from 25 July 2018 to 28 October 2018 (96 days) were estimated from discharge data of the Ficarolo station (FCR), which is positioned  $\sim 20$  km upstream from Pontelagosuro (Figure 1) and shows highly comparable discharge  $Q$  values (slope = 0.98,  $R^2 = 0.99$ , Figure S3).

Precipitation (PPT) data were extrapolated from E-OBS data files from the Copernicus Climate Change Service (<https://surfobs.climate.copernicus.eu/>, accessed on 2 October 2023) [68]. An E-OBS data file is composed of daily raster files, including the modelised European precipitation at a  $0.1^{\circ}$  regular grid resolution. The precipitation data represent the sum of the amount of rain, snow and hail measured as the height of the equivalent

liquid water in a square meter. The daily average precipitation was calculated at the basin scale and then summed to obtain the monthly and annual mean precipitation.

### 2.3. Calculation of Exported Loads and Export Metrics

Nutrient loads were calculated on a monthly and annual basis as the product of the discharge-weighted mean concentration and the mean discharge of the period [69], as follows:

$$L = \frac{\sum_{i=1}^n c_i \times Q_i}{\sum_{i=1}^n Q_i} \times \bar{Q} \times k \quad (1)$$

where

$L$  = period loading ( $\text{kg time}^{-1}$ );

$c_i$  = concentration on day <sub>$i$</sub>  ( $\text{g m}^{-3}$ );

$Q_i$  = mean daily discharge on day <sub>$i$</sub>  ( $\text{m}^3 \text{s}^{-1}$ );

$\bar{Q}$  = mean period discharge ( $\text{m}^3 \text{s}^{-1}$ );

$k$  = temporal factor to calculate period  $L$ .

We assessed the nutrient export scheme for each month, applying concentration–discharge metrics [61,70] across years according to the following power law relationship [71]:

$$c = aQ^b \quad (2)$$

$$\ln(c) = \ln(a) + b \ln(Q) \quad (3)$$

where  $\ln(a)$  is the intercept and  $b$  the slope of the  $\ln(c) - \ln(Q)$  regression.

The slope of the  $\ln(c) - \ln(Q)$  relationship describes the export pattern: a positive slope ( $b > 0$ ) indicates an enrichment pattern, while a negative slope ( $b < 0$ ) means a dilution pattern. When the  $\ln(c) - \ln(Q)$  relationship presents a not significant slope ( $b \approx 0$ ), Thompson [70] proposed to associate the ratio between  $c$  and the  $Q$  coefficient of variation ( $CV$ ), as a measure of the relative variability between  $c$  and  $Q$  irrespective of the correlation:

$$\frac{CV_c}{CV_Q} = \frac{Q}{c} \frac{\sigma_c}{\sigma_Q} \quad (4)$$

According to previous published works, we distinguished chemostatic behaviour (low ratio,  $CV_c/CV_Q < 0.5$ ) from chemodynamic behaviour (high ratio,  $CV_c/CV_Q > 0.5$ ), which is considered as an index of high solute reactivity or threshold-driven transport [33,61].

Precipitation, runoff and the exported loads during summer months were also explored through a comparison between dry and wet years. First of all, the PPT- $Q$  relationship was analysed with a quartile analysis, which allowed a partitioning of the dataset in dry, wet and normal years. The first quartiles of both PPT and  $Q$  were assumed to be the upper thresholds of dry years, the 3rd quartiles were the lower thresholds of wet years, and the 25th–75th interquartile comprised the normal years. Then we grouped the months according to Montanari [51] in order to represent periods of the year that are characterised by the critical patterns of both hydrological and biogeochemical processes.

### 2.4. Statistical Analyses

All the statistical analyses were performed using R software [72]. To test the significance of monthly variability for PPT,  $Q$  and nutrient concentrations, we applied a one-way ANOVA through the *lm* function under the R Programming Language [72]. Differences between months were estimated with the summary function, verifying the contrast against January values. To ensure the model assumptions were met and due to the skewness of the distribution of residuals, data were log- or square root-transformed on the basis of the graphical evaluation of *QQplots*.

The PPT and  $Q$  relationship and the concentration and  $Q$  relationship were analysed at the annual level and for each month with a linear regression model of log-log-transformed data.

To assess long-term patterns and the periodicity within the year of nutrient loads, we applied a *Generalised Additive Mixed Model* (GAMM) with the R package *mgcv* [73]. To verify the significance of monthly trends, months were treated as a factor, and then we tested the general model with an annual common smoother, plus monthly level smoothers with a different wiggleness, as follows:

$$y_i \sim month + s(year) + s(year, by = month) + \varepsilon_i \quad (5)$$

A reduction in collinearity between the reference smoother and monthly trends was achieved by specifying the marginal TPRS basis as described by Pedersen [74]. In order to ensure that model assumptions were met and due to the skewness of the distribution of residuals, data were log- or square root-transformed on the basis of the graphical evaluation of *QQplot*, while to resolve the temporal autocorrelation we used the *corARMA* function within the *mgcv* R package [73]. Finally, the autoregressive order ( $p$ ) varied from 1 to 10, and we then selected the model with a lower *AIC* (Akaike Information Criterion) [75]. As a spline function, we adopted the cubic regression ( $bs = "cr"$ ). The accepted model was finally calculated using the *Restricted Maximum Likelihood* (REML) [75].

### 3. Results

#### 3.1. Temporal Variability of Precipitation, Hydrology and Nutrient Concentration

Over the last three decades (1992–2022), the total annual precipitation (PPT) in the River Po basin ranged from 673 (2022) to 1286 (2014) mm, with the median = 1029 mm and mean =  $918 \pm 169$  mm (Figure 2A). Concurrently, at the closing section of the River Po basin (Pontelagoscuro), the mean annual discharge (Q) varied from 550 (2022) to 2282  $\text{m}^3 \text{s}^{-1}$  (2014), with the median = 1443  $\text{m}^3 \text{s}^{-1}$  and mean =  $1450 \pm 409$   $\text{m}^3 \text{s}^{-1}$  for the whole period (Figure 2A). Both PPT and Q underwent a significant intra-annual variability (ANOVA,  $p < 0.001$ ), which can be synthesised by two-phase seasonal patterns (Figure 2B). The higher PPT periods occurred from April to June, and from August to November, when they attained significant peaks, i.e.,  $90 \pm 40$  mm in May and  $118 \pm 77$  mm in November. By contrast, the lowest values were detected in February ( $49 \pm 35$  mm) and July ( $61 \pm 23$  mm). Similarly, Q attained two significant peaks ( $t$ -test,  $p < 0.001$ ) in May ( $1985 \pm 1190$   $\text{m}^3 \text{s}^{-1}$ ) and November ( $2204 \pm 1735$   $\text{m}^3 \text{s}^{-1}$ ). Significantly lower values ( $t$ -test,  $p < 0.01$ ) were detected in July and August ( $850 \pm 405$   $\text{m}^3 \text{s}^{-1}$ ), while the Q was relatively constant from January to April ( $1381 \pm 684$   $\text{m}^3 \text{s}^{-1}$ ) (Figure 2B).

Based on the combination of quartile analysis outcomes of both PPT and Q, six very dry years were identified from 2000 onwards. Moreover, five of the six wettest years fell in the same period, evidencing a huge amplification of hydrological variability (Figure 2A). Table 1 shows the comparison of river discharge rates under the extreme conditions of the wettest (2014) and driest (2022) years and with the mean values of the whole period from 1992–2022.

**Table 1.** Main water fluxes ( $\text{km}^3 \text{yr}^{-1}$ ) from 1992 to 2022 in the River Po basin. The mean and the extreme conditions of flood (2014) and drought (2022) are considered. PPT: total annual precipitation; Q: annual river discharge measured at Pontelagoscuro (river basin closure).

Years	PPT ( $\text{km}^3 \text{yr}^{-1}$ )	Q ( $\text{km}^3 \text{yr}^{-1}$ )
Wettest (2014)	93.6	72.0
Mean (1992–2022)	68.0	45.7
Driest (2022)	51.0	17.3

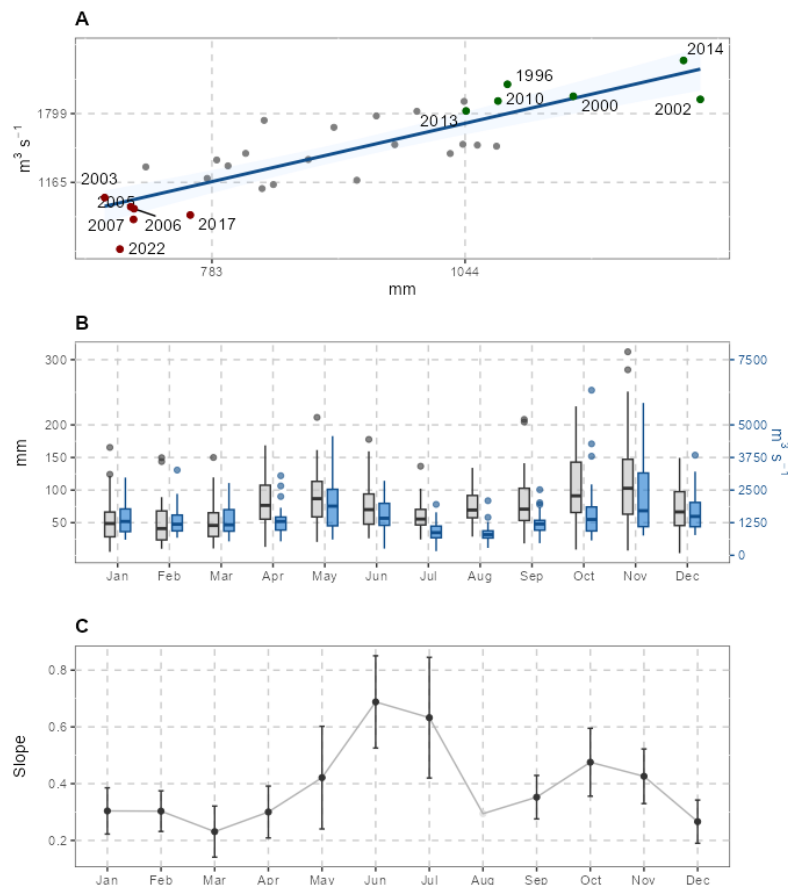


**Figure 2.** (A) Relationships between the annual cumulated precipitation (PPT) and the mean annual water discharge (Q) in the River Po basin. Dashed lines represent the first and third quartiles of both PPT and Q. Red dots represent dry years, while green dots represent wet years. (B) Boxplot of monthly cumulated PPT (grey) and monthly mean Q (blue); whiskers represent 5th and 95th percentiles, boxes the 25th and 75th percentiles, horizontal lines the 50th percentile. (C) Slope  $\pm$  st. error of  $\ln(Q) - \ln(PPT)$  regression, with Q = mean monthly water discharge and PPT monthly cumulated precipitation; black dots represent significant slopes ( $p < 0.05$ ). Expanded plots of monthly relationships are available in Figure S4 and statistics in Table S1.

Moreover, Q was significantly correlated to PPT, with  $r = 0.85$  and  $p < 0.0001$ . The PPT and Q relationships analysed for each month indicate a significant slope for all months except for August. The slope peaked in June–July ( $b = 0.73$ – $0.77$ ) and was lower during the rest of the year ( $b = 0.25$ – $0.47$ ) (Figures 2C and S4, Table S1).

At the basin scale, in both wet and dry years, approximately 50% of PPT is recorded between May and October, with minimum values in summer (Table S2). The ratios between the quantities of water falling to the ground during wet and dry years (WET/DRY) in the different periods considered are relatively low and constant (1.2–1.5). The river flow presents a similar trend to that of precipitation, but with a significantly higher WET/DRY ratio (2.3–2.9) (Table S2).

The concentrations of the main N and P compounds undergo a wide variability with a clear seasonality, especially for nitrate ( $\text{N-NO}_3^-$ ) and SRP (Figure 3). On average,  $\text{N-NO}_3^-$  concentrations decrease from January ( $\sim 3 \text{ mg N L}^{-1}$ ) to July ( $\sim 1.3 \text{ mg N L}^{-1}$ ), and grow in the second part of the year. Moreover,  $\text{N-NO}_3^-$  accounts for 93–98% of dissolved inorganic nitrogen ( $\text{DIN} = \text{N-NO}_3^- + \text{N-NH}_4^+$ ), while the contribution of ammonium ( $\text{N-NH}_4^+$ ) is almost negligible for most of the year. Unlike SRP, TP attains very high concentrations in May and from October to December (95th percentile  $> 0.3 \text{ mg P L}^{-1}$ ) mainly due to flood events, while monthly medians vary between 0.13 and 0.16  $\text{mg P L}^{-1}$ . The molar DIN:SRP ratio is usually very high, evidencing a shortage of SRP vs. DIN.

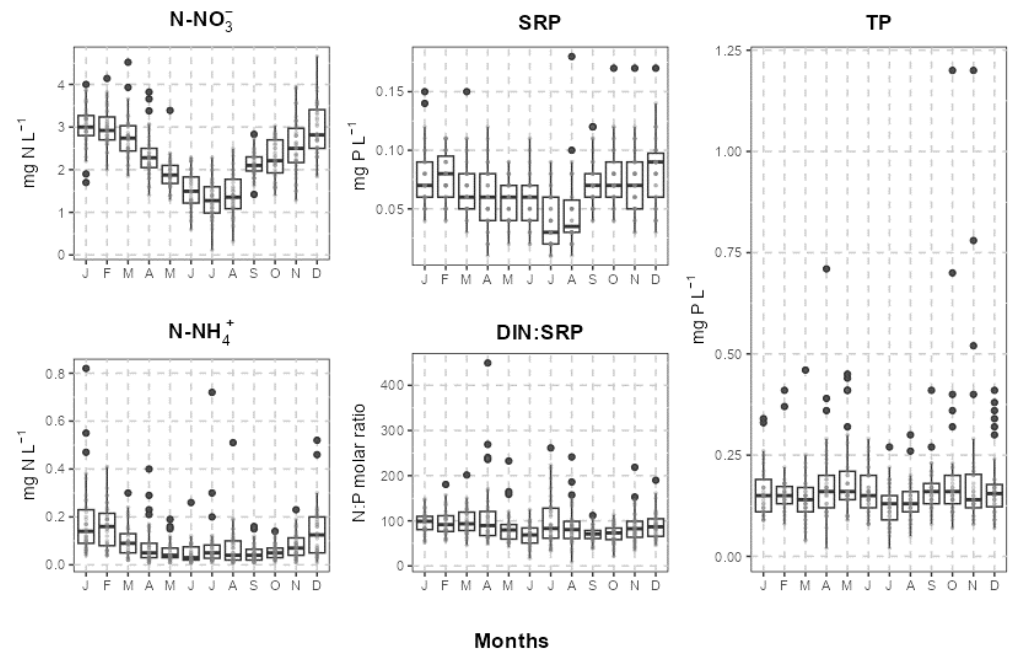


**Figure 3.** Monthly variations in the concentrations of nitrate ( $\text{N-NO}_3^-$ ), ammonium ( $\text{N-NH}_4^+$ ), soluble reactive phosphorus (SRP), total phosphorus (TP), and DIN:SRP molar ratio between 1992 and 2022. Whiskers represent 5th and 95th percentiles, boxes the 25th and 75th percentiles, horizontal lines the 50th percentile.

### 3.2. Temporal Variability of Nutrient Loadings

Nutrient loadings exported from the River Po to the Northern Adriatic Sea undergo clear temporal patterns, both within the same year and over three decades, from 1992 till 2022 (Figure 4).

The DIN loading variations over the year conform to those of  $\text{N-NO}_3^-$ , which attain significantly lower values from June to September ( $p < 0.001$ ). The  $\text{N-NH}_4^+$  loadings are almost negligible over the year (from March to November) and they account for up to 10% of the DIN only during flood events. The TP loading usually attains two peaks in May ( $p < 0.01$ ) and November ( $p < 0.01$ ), while it is persistently low at low Q rates. Finally, SRP exhibited an intermediate behaviour between  $\text{N-NO}_3^-$  and TP, with lower loadings in July and August ( $p < 0.001$ ) and higher loads in November ( $p < 0.05$ ) and April ( $p = 0.05$ ). The DIN:SRP molar ratio shows a two-phase trend, with low values in June ( $p < 0.001$ ) and September–October ( $p < 0.001$ ).

Over the long-term period, from 1992 to date,  $\text{N-NO}_3^-$  and SRP are more conservative ( $\text{CV} = 0.65$ ) than TP ( $\text{CV} = 1.6$ ), while  $\text{N-NH}_4^+$  has an intermediate behaviour ( $\text{CV} = 1.0$ ). The annual reference–smooth term decreases progressively and is statistically significant for  $\text{N-NO}_3^-$  ( $p < 0.01$ ),  $\text{N-NH}_4^+$  ( $p < 0.001$ ) and TP ( $p < 0.01$ ), while SRP changes are not statistically significant (Figure 4). Moreover, the observed patterns suggest the nitrate decline started in the 1990s. The DIN:SRP molar ratio is also undergoing a significant decrease, especially in the last decade.

Single monthly smooths vary by nutrient and in some cases also by month. The period from November to May and September show the same decreasing trend for  $\text{N-NO}_3^-$ . The June to July period and October present a significantly different trend ( $p_{\text{Jun-Aug}} = 0.001$ ,  $p_{\text{Oct}} < 0.05$ ) than the general smooth: June and October are characterised by a greater decrease in the first decade and then became stable in the last two decades, while August generally shows no temporal trend. Our findings show that the period with the minimum  $\text{N-NO}_3^-$  load, usually occurring in summer, varies in intensity and temporal extension. The decreasing phase is progressively anticipated (from Jun–Jul to May–Jun); then the minimum (which is reached in July rather than in August) becomes more pronounced. Finally, the return to the standard autumnal load is delayed from September–October to



October–November. Therefore, the seasonal curve corresponding to summer becomes flatter and larger than in the 1990s.

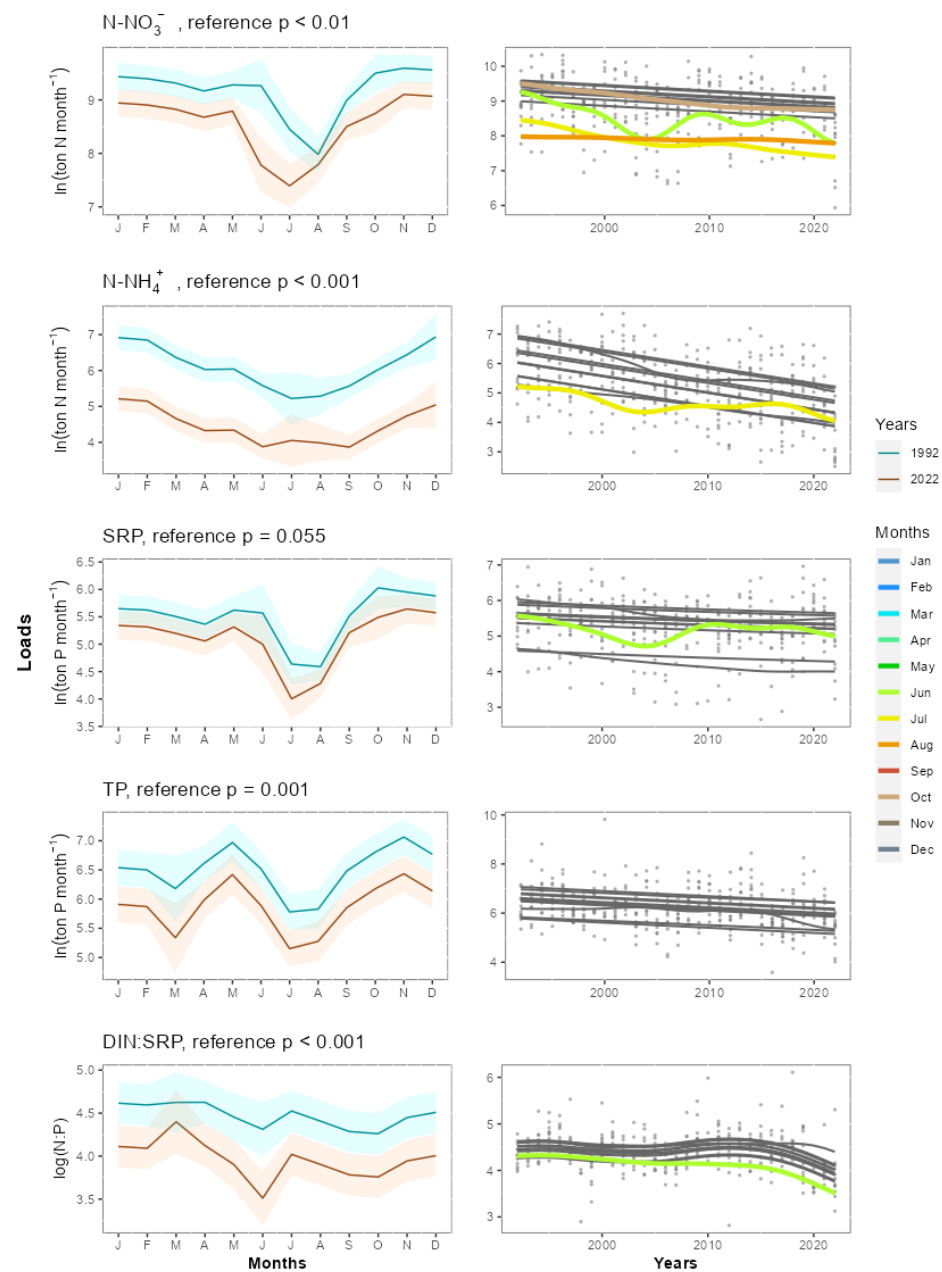


**Figure 4.** Temporal trends of  $\text{N-NO}_3^-$ ,  $\text{N-NH}_4^+$ , SRP, TP and DIN:SRP molar ratio. **Left panel:** Modelled monthly trends in 1992 and in 2022. **Right panel:** Long-term trend for each month. Coloured lines follow trends that are different from the reference patterns. Linewidth indicates the statistical significance value: thin lines are not significant, wide lines are significant at  $p < 0.05$ . Nutrient loads are showed on a ln scale. Please note differences in y scales between graphs.

For  $\text{N-NH}_4^+$ , only December and July present a significantly different smooth ( $p < 0.05$ ) from the general one, with a higher decreasing rate for December in the first decade and a stabilisation of the load in July. Log transformation evidenced that the larger  $\text{N-NH}_4^+$  loss is concentrated during the coldest period (Oct–Mar).

Similarly, TP presents no different smooths among months, while log transformation also indicates that the larger losses occur during wetter months (May, Oct–Dec). On the contrary SRP shows a pattern similar to  $\text{N-NO}_3^-$ , but less significant. The decreasing

load of June ( $p = 0.01$ ) confirms the minimum anticipation, while the weaker ( $p = 0.06$ ) significance of the October rate may suggest an autumnal shift, as for  $N-NO_3^-$ .

Finally, the significance of the molar DIN:SRP ratio is strongly dependent on the trend of the last decade, confirming the steady decrease in  $N-NO_3^-$  against the more fluctuating trend of SRP. Coherently with the results of  $N-NO_3^-$  and SRP, the DIN:SRP also diverges from the reference trend in June ( $p < 0.05$ ), with a higher decrease rate.

### 3.3. Loading Responses to Precipitation

Load–precipitation relationships calculated on annual data are reported in Table 2 and Figure S5.

The general slope is highly significant for all nutrients, except for the DIN:SRP molar ratio. The monthly relationships between load and precipitation show a similar behaviour for  $N-NO_3^-$ , SRP and TP, with decreasing slopes from summer to autumn and lower or non-significant values from winter to early spring (Figures 5 and S6 and Table S3). Despite TP and SRP being similar, the values of the TP slope are less variable between months, indicating a more stable response to rainfall. For  $N-NH_4^+$ , the slope is non-significant for 8 out of 12 months, except for the wettest months (May, and September to November). The slope of the DIN:SRP molar ratio is non-significant for most of the year, except in July and November.

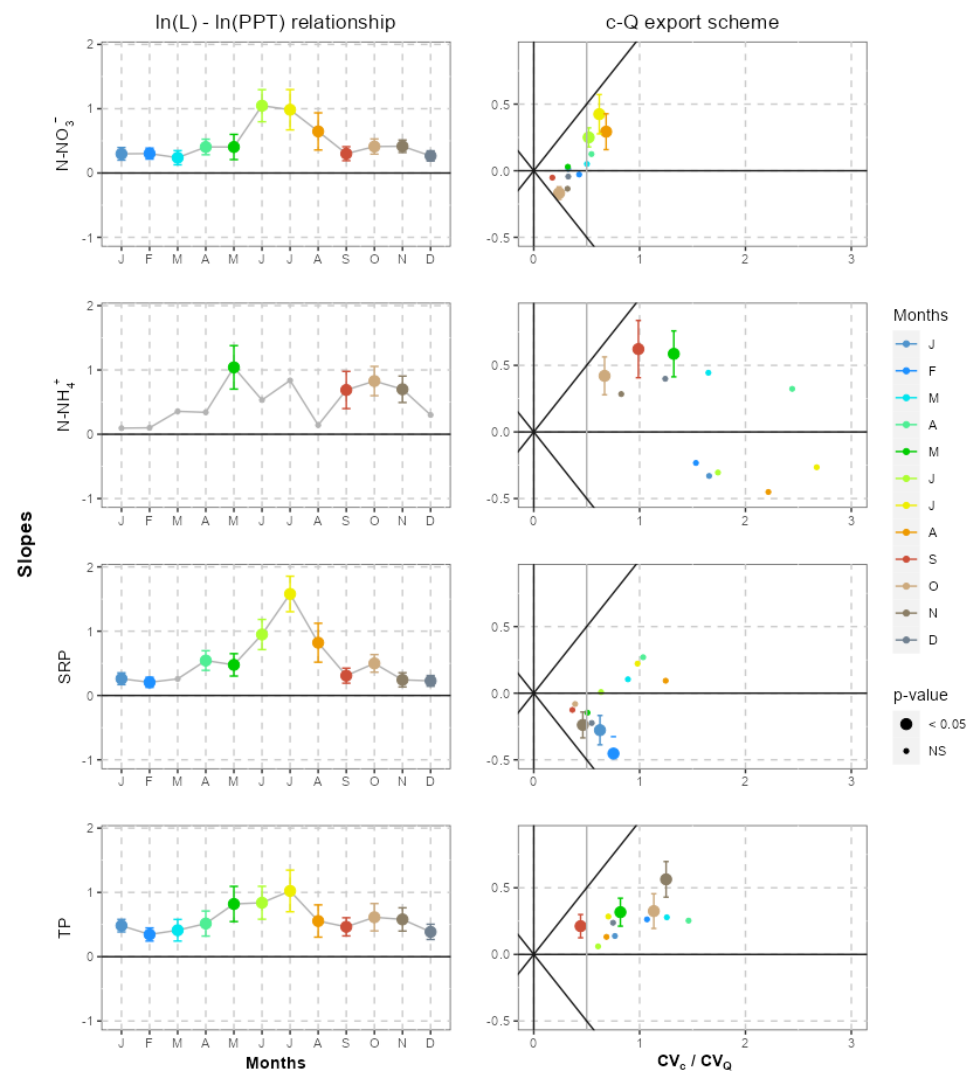


**Figure 5.** Left panel: Slope  $\pm$  st. error of the  $\ln(L)$ - $\ln(PPT)$  relationship between precipitation versus nutrient loads. Dot size represents the significance of the slope (expanded plots of monthly relationships)

can be found in Figure S6 and statistics in Table S3). **Right panel:** Export regime scheme as described by Musolff [61]. The slope  $\pm$  st. error of the  $\ln(c)$ - $\ln(Q)$  relationship is reported on the y axis; the  $CV_C/CV_Q$  ratio is reported on the x-axis. Dot size represents the significance of the  $\ln(c)$ - $\ln(Q)$  slope. A negative slope ( $b < 0$ ) indicates a dilution pattern, while a positive slope ( $b > 0$ ) indicates a mobilisation regime. When  $b \approx 0$ , the solid grey line ( $x = 0.5$ ) indicates the theoretical boundary that differentiates chemostatic from chemodynamic behaviour. Expanded plots of monthly relationships can be found in Figure S8 and statistics in Table S4.

In dry years from May to October, the  $N\text{-NO}_3^-$  load, which represents nearly 95–98% of the reactive N, is 31% of the annual total and does not exceed 15% from June to September (Figure 6 and Table S2). A similar trend also occurs in wet years, but with a WET/DRY ratio between 2.5 and 4.0 in June–August. SRP and TP (Figure 6 and Table S2) present trends similar to those of  $N\text{-NO}_3^-$ .

**Table 2.** Relationship between nutrient load (L) and precipitation (PPT) at the yearly scale (plots can be found in Figures S5 and S6) and between nutrient concentration (c) and water discharge (Q) at the monthly scale (plots can be found in Figures S7 and S8). Significance is shown with asterisks ( $p < 0.05$  \*,  $p < 0.01$  \*\*,  $p < 0.001$  \*\*\*).

Relationships	Parameter	Slope	St. Error	R <sup>2</sup>
$\ln(L) - \ln(PPT)$ annual data	$N\text{-NO}_3^-$	1.20 ***	0.24	0.47
	$N\text{-NH}_4^+$	1.73 ***	0.48	0.31
	SRP	0.93 ***	0.20	0.42
	TP	2.02 ***	0.35	0.53
$\ln(c) - \ln(Q)$ monthly data	$N\text{-NO}_3^-$	0.18 ***	0.03	0.06
	$N\text{-NH}_4^+$	0.15 *	0.08	0.01
	SRP	0.08 *	0.04	0.01
	TP	0.29 **	0.04	0.13

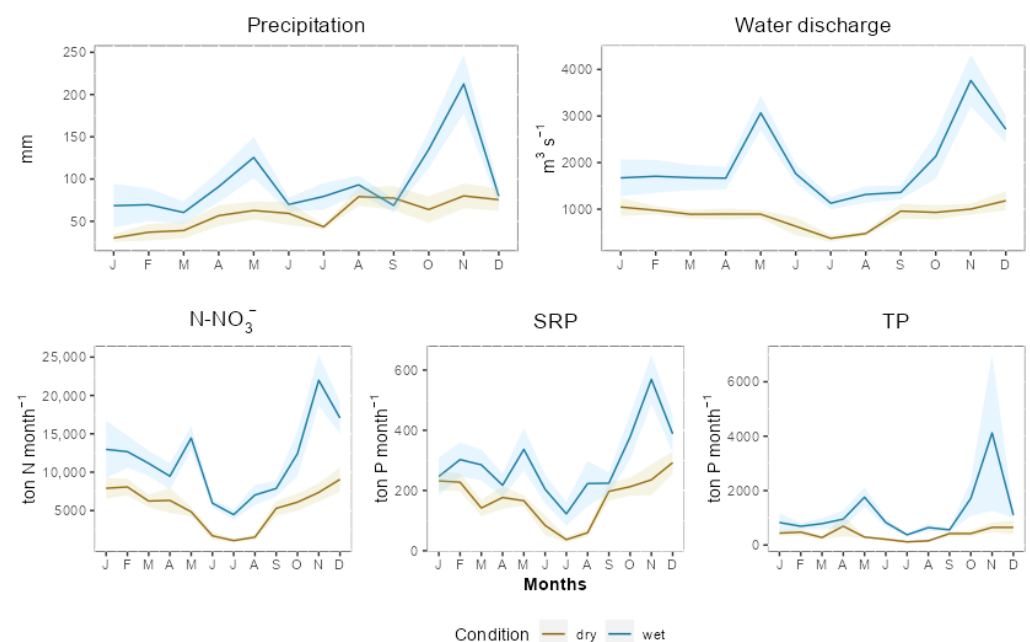


**Figure 6.** Average  $\pm$  st. error values of precipitation, water discharge,  $N\text{-NO}_3^-$ , SRP and TP during wet and dry years based on the classification proposed in Figure 2A.

### 3.4. Concentration–Water Discharge Metrics

The concentration–discharge (c-Q) relationships calculated with the whole dataset are reported in Table 2 and Figure S7. The general slope is significant for all nutrients, with the following pattern:  $TP > N\text{-NO}_3^- > N\text{-NH}_4^+ > SRP \approx \text{DIN}$ : SRP. The c-Q relationship was

also tested for each nutrient by month (Figures 5 and S8 and Table S4), to assess whether the relationship is constant throughout the year or if it is season-dependent.

The TP monthly slope ( $b$ ) is overall positive throughout the year, although it is statistically significant only in May and from September to November, indicating the dominance of the mobilisation regime. By contrast, the N-NO<sub>3</sub><sup>-</sup> slope is not statistically significant during winter and spring, while from June to August it is characterised by a mobilisation pattern ( $b > 0$ ), and during October and November it follows a dilution behaviour ( $b < 0$ ). The concentration of N-NH<sub>4</sub><sup>+</sup> and SRP appears to be largely independent of water discharge, except in May, September and October, when a mobilisation pattern of ammonium occurs, with a significant dilution pattern for SRP in colder months (November, January and February). As a clear consequence, the DIN:SRP molar ratio appears to be largely independent from  $Q$ . The only exception is during the colder months (January and February), where the slope becomes statistically significant ( $p_{\text{Jan}} = 0.01$ ,  $p_{\text{Feb}} = 0.001$ ) and varies from 0.16 in December to 0.32 in February. This trend is mostly driven by the dilution pattern of SRP, because the N-NO<sub>3</sub><sup>-</sup> concentration does not change with the discharge during these months.

The  $CV_C/CV_Q$  ratio pinpoints three main groups at the interannual scale: (i) nearly chemostatic behaviour ( $CV_C/CV_Q < 0.5$ ) for N-NO<sub>3</sub><sup>-</sup> (0.48), (ii) chemodynamic behaviour ( $CV_C/CV_Q > 0.5$ ) for SRP (0.59) and TP (0.9), and (iii) highly chemodynamic behaviour ( $CV_C/CV_Q > 1$ ) for N-NH<sub>4</sub><sup>+</sup> (1.45). N-NH<sub>4</sub><sup>+</sup> and TP also present, respectively, highly chemodynamic and a chemodynamic behaviour at monthly scale. SRP shows general chemodynamic behaviour except in September and October, which are characterised by chemostatic behaviour. Finally, for N-NO<sub>3</sub><sup>-</sup> we observed chemostatic behaviour except in July and August.

#### 4. Discussion

In this work, we analyse changes in the N and P loadings exported by the River Po to the Northern Adriatic Sea over short-term (months and seasons) and long-term (three decades from 1992 till 2022) temporal scales. The main goal is to elucidate the effects of precipitation on the concentration and loadings of N-NO<sub>3</sub><sup>-</sup>, N-NH<sub>4</sub><sup>+</sup>, SRP and TP. We also evaluate the basin export regime in order to infer the major drivers that control the loads, i.e., hydrological, geochemical and biogeochemical patterns. These are understudied but important issues in inland waters to support effective basin management and the protection of downstream water bodies, as they can provide new insights into the capacity of basins to retain and export nutrient loads under heavy exploitation along with climate and hydrology changes.

##### 4.1. Decreasing Load Trends Are Driven by Changes in Hydrology and Seasonality

The long-term analysis shows a general decreasing trend in nutrient loads, which is higher for N-NH<sub>4</sub><sup>+</sup> than for N-NO<sub>3</sub><sup>-</sup> and TP, while reactive phosphorus shows no clear decrease over the last 30 years. This is not unexpected, as other studies have already described such a decrease in nutrient loads in the Po basin and in other basins [12,56,58,76,77].

In the River Po basin, since the 1970s, nutrient loadings have been managed primarily through environmental policies aiming to implement urban wastewater processing and the removal of polyphosphates from detergents. These policies have been successful, especially for the reversal of the reactive P-loading trend in the 1980s, but they were less effective in the reduction of N and TP loads [12], similarly to the Elbe, Danube and Rhone rivers [54,76,77]. Since nitrogen loadings are generated by diffuse agricultural sources and by atmospheric deposition, they are in fact much less affected by policies and the management of wastewaters [12]. At the same time, TP loads are sustained by particulate P export driven by land erosion and the delayed release of P accumulated in agricultural soils [78]. Our analysis evidences that the long-term trend is clearly affected by seasonal events, and the decrease rate differs between months. The N-NO<sub>3</sub><sup>-</sup> load decrease is mainly concentrated in the summer dry period due to a steeper minimum in July, along with an

amplification from 3 up to 5 months of the summer dry period duration. The persistence of dry conditions (June to October) largely contributes to the annual load reduction. The TP decrease, despite similar summer minima, also depends on the reduction of the spring and autumn flooding phases. The  $\text{N-NH}_4^+$  trend is also unequally distributed among months with a larger decrease in winter, but it is less impacting as it contributes less than 5% of the DIN loading. Therefore, over the last 30 years, the nutrient loads originating from diffuse sources in farmland are likely to be mainly controlled by seasonal variations in PPT, hydrology and biogeochemical processes in the river and its catchment [9]. As such, the understanding and management of the nutrient loadings delivered to the Adriatic Sea by the River Po is challenged by the huge variability in river discharge in the last two decades, which is due to changes in precipitation patterns and direct water use.

The mean water fluxes estimated for the 1992–2022 period (Table 1) are close to those estimated by Montanari [66] for 1960–1990. In fact, we found  $\text{PPT} = 68 \text{ km}^3 \text{ yr}^{-1}$  and  $Q = 45.7 \text{ km}^3 \text{ yr}^{-1}$  (this study) vs.  $\text{PPT} = 78 \text{ km}^3 \text{ yr}^{-1}$  and  $Q = 47 \text{ km}^3 \text{ yr}^{-1}$  [66]. However, in the latter period, the flux ranges are extremely variable, oscillating from a maximum in 2014 ( $72.0 \text{ km}^3 \text{ yr}^{-1}$ ) to a nearly four-fold lower dramatic minimum in 2022 ( $17.3 \text{ km}^3 \text{ yr}^{-1}$ ). The very low  $Q$  flux in 2022 is equivalent to the total flux quota for agriculture in normal years [66], which highlights a critical water shortage. The River Po basin is characterised by a biphasic precipitation pattern, which corresponds to a biphasic water discharge, as described by Montanari [66]. At a multi-year scale, significant relationships emerge between precipitation and flow, which vary by year and season, with the form of precipitation being responsible for this relationship. For instance, from winter to early spring, snowfall and snowmelt contribute to accumulating solid water, thus controlling the high spring discharge. In fact, precipitation is stored as snow on the Alps during the winter season, and then it is released from spring to early summer, contributing to the Po flood during this period [79]. On the contrary, the discharge response to precipitation is immediate in the case of rainfall and can reach peaks during summer storms. In this season, discharge rates are low and the runoff can undergo sudden variations induced by short-term intense rainfalls, indicating that PPT has greater effects on the  $Q$  itself than in the other months. Furthermore, high fluxes can be also sustained by the lower water demand for irrigation which follows rain events. The annual decline in the River Po discharge in summer is more accentuated than the declining rate of the annual precipitation regime (Table 1). This means that in dry years, the water deficit is caused not only by the decrease in precipitation but also by other factors, such as the increase in evaporation and evapotranspiration, which in turn are enhanced by the increasing irrigation withdrawals [51].

Modifications in the hydrological regime are associated with changes in nutrient loads, particularly during the summer months when reductions in runoff enhance the load reductions. Under drought conditions, the loadings exported to the Adriatic Sea (i.e.,  $\text{DIN} = 38,690 \text{ t N yr}^{-1}$ ,  $\text{SRP} = 1690 \text{ t P yr}^{-1}$ ,  $\text{TP} = 2721 \text{ t P yr}^{-1}$ ) are far below the values in the pristine river [12]. In June–August, with low to absent precipitation, we found a marked decrease in the  $\text{N-NO}_3^-$  and TP loads, which, in dry years, are four times lower than in wet years. Such decreases can be due to both lower land to water connectivity and to the higher river metabolism, which tends to increase under dry and warm conditions when land inputs are minimal and fluxes are lower (see below). Therefore, nutrient loadings are very low in summer, when physical conditions (solar radiation, temperature) are optimal for marine primary production. This asynchrony between chemical and physical factors might generate a sort of biogeochemical mismatch between nutrient availability and primary production, playing a key role in determining the evolution of the biodiversity, productivity, food webs and trophic state of the Northern Adriatic Sea, which seemed to undergo oligotrophication during the harsh and long drought in the 2003–2007 period [80–83]. On the other side, a few years later (2010 till 2015) a very variable and wet phase occurred [84]. In the very wet 2014, the loadings exported by River Po (i.e.,  $\text{DIN} = 145,849 \text{ t N yr}^{-1}$ ,  $\text{SRP} = 3899 \text{ t P yr}^{-1}$ ,  $\text{TP} = 15,721 \text{ t P yr}^{-1}$ ) were similar to those detected from the mid-1970s to the 1980s, when the Northern Adriatic coast was impacted by unprecedented

eutrophication [12]. This pattern brings up new questions on the legacy of nutrients, regarding, for instance, the sudden release of N and P stored in agricultural soils and in surface sediments in the past decades [15].

#### 4.2. Hydrology Controls Load Export

The analysis of the relationships between precipitation and loads demonstrates that the precipitation pattern drives the exported load at seasonal time scales, with different behaviour for the diverse chemical forms of N and P. The different precipitation effects on the exported load can be explained by seasonal changes in hydrological connectivity and the relationship between concentration and discharge and whether the load is driven only by discharge (e.g., a dilution pattern) or also by concentration increases (e.g., the effect of erosion, soil weathering and leaching). Solutes from deep bedrock usually follow a dilution behaviour, whilst solutes with a surface genesis (e.g., litter and upper soil layers) follow enrichment patterns [50]. Chemostatic behaviour has been attributed to the homogenous and uniform distribution of elements in the catchment, meaning that changes in hydrological connectivity and the flow path do not affect solute concentrations, as the load is dependent on the increase in the discharge.

In the River Po, from June to August, rainfall from summer storms increases the nitrate and phosphorus loads, but the underlying mechanisms are likely to be different. Nitrates undergo a clear mobilisation behaviour, while SRP and TP concentrations do not show a clear relationship with discharge, but a high chemodynamic pattern, along with  $\text{N-NH}_4^+$ . Positive relationships between concentration and discharge have been attributed to the reconnection of surface or subsurface catchment components where a given element is more abundant, and/or to enhanced erosion during high flows for suspended sediment and the associated pollutants [85,86]. In summer, hydrological disconnection favours the accumulation and retention of  $\text{N-NO}_3^-$  in the soil or in the riverbeds [11,87]. Summer storms might cause intense rainfall, leading to runoff that suddenly reconnects the hydrological network, thus mobilising and exporting the accumulated  $\text{N-NO}_3^-$ , especially in heavily exploited farmlands [88–90].

The lack of an enrichment pattern for the other nutrients suggests that hydrological reconnection and solute mobilisation are not the most relevant mechanisms during summer. When the  $\ln(c)-\ln(Q)$  slope is not significant, the variability in concentration against discharge ( $CV_C/CV_Q$ ) indicates a degree of nutrient transformation along the continuum [50]. During summer, SRP and  $\text{N-NH}_4^+$  show strong chemodynamic behaviour, which may depend on biological control processes [61]. A low flow and high light availability support the stream metabolism and phytoplankton growth, which removes reactive P and  $\text{N-NH}_4^+$  from the water column, decreasing their concentrations [91,92]. The high variability in concentration is expected to mask the mobilisation effect of SRP in summer, which, similarly to  $\text{N-NO}_3^-$ , seems to be more easily exported during floods [93,94]. The assimilation of SRP could also favour an increase in TP during low flow conditions, thus weakening the strong hydrological dynamics of TP dependant on the erosion of particulate P, as TP concentrations typically show a positive relationship with discharge [27,60]. Nitrate may also be under biological control, as confirmed by its weak chemodynamic behaviour combined with low concentrations during low flow [60]. In summer, a lower water velocity and higher temperature could promote not only denitrification [58] but also consumption by primary producers, similar to what has been described for the Elbe basin [95].

During autumn and in May, which are the wettest periods of the year, both TP and  $\text{N-NH}_4^+$  show an enrichment pattern that enhances the role of precipitation in the export rate, in contrast to the other months. While for TP this aspect is quite predictable due to the erosion effect of rainfall on the P particulate form (particularly in heavily impacted basins [27,96,97]), this pattern is less predictable for  $\text{N-NH}_4^+$ . However, this appears to be consistent with Tesi [98], who found that in the River Po ammonia was positively correlated with suspended sediment (which increases during high flow events). The authors also suggest  $\text{N-NH}_4^+$  concentrations to be driven by either microbial activity (ammonification–

nitrification) or ionic exchange, the rates of which are proportional to suspended sediment concentrations. Finally, the observed chemodynamic behaviour associated with positive slopes in autumn and May is likely linked to a threshold-driven transport-dependant pattern. The activation of differently distributed sources can be related to the geological spatial heterogeneity for TP, but opens further issues for N-NH<sub>4</sub><sup>+</sup> [61], such as the role of combined sewer overflows. Combined sewer systems represent the most common form of sewage collection in urban areas [99]. In these systems, sanitary waters are the primary source of sewage discharge during dry conditions. However, during periods of heavy precipitation, the conveyance capacity of the sewer network or the treatment plant processing capacity may be exceeded, resulting in the discharge of partially treated and/or raw sewage into surface waters due to sewer overflow [99].

The opposite behaviour of N-NO<sub>3</sub><sup>-</sup> and SRP in winter, also confirmed by the DIN:SRP ratio, remains partly unexplained. The SRP dilution pattern with increasing flow rate predominates in winter and is consistent with the dilution of point sources [100,101]. On the contrary, the N-NO<sub>3</sub><sup>-</sup> chemostatic behaviour observed from November to April indicates a large nitrate legacy store, typical of heavily exploited basins and suggesting the absence of spatial differences in soil water and groundwater concentrations [102,103]. The absence of a correlation between the N-NO<sub>3</sub><sup>-</sup> concentration and discharge has been attributed to a spatial separation between the discharge-generating zones and solute source areas [103,104]. This dynamic can be explained by the distribution of the most abundant precipitation patterns and the differential human pressures along the River Po basin, with the former generally positioned in the natural mountain sector of the catchment and the latter found in the anthropised urban areas and cropland [12,66].

These results demonstrate that a substantial amount of information regarding the factors that regulate the formation of nutrient loads can be obtained by examining the relationships between concentration and discharge. Nevertheless, the comprehension of river basin hydro-biogeochemical dynamics and the relative significance of meteorological, biological and geological processes is complex due to the fact that these processes occur at different temporal scales [60,61,90]. In this work, we used concentration data collected at sampling frequencies ranging from fortnightly to monthly. This discrete sampling frequency enabled us to gain insights into how precipitation patterns differently influence the interannual and seasonal dynamics of N and P loads. However, this sampling frequency is not sufficient to capture short-term, event-scale dynamics, which limited our ability to disentangle the relative importance of specific processes or identify control points of nutrient transport at the fine scale. Future studies integrating different sampling frequencies would help to identify the different drivers that regulate N and P load formation across different temporal scales and determine their relative importance.

## 5. Synthesis and Perspectives

In the River Po basin, precipitation patterns can explain the changes observed in the nutrient loads exported to the Northern Adriatic Sea at both an annual and seasonal scale. However, the effect of this tendency varies by month and nutrient form due to the different relations between precipitation and discharge and different seasonal concentration regimes.

The relationship between PPT and Q pinpointed six very dry and five very wet years in the last two decades, with an increased frequency of opposite extremes of water discharge and nutrient loadings. Given the predictions of the progressive tropicalisation of the Mediterranean climate, one can envisage a scenario with less snowfall and snow accumulation, with a consistent decrease in the snowmelt that is currently regulating the river discharge in late spring and early summer [34,36,66]. Furthermore, the water discharge will be more dependent on rainfall—especially short-term heavy rainfall—thus exacerbating the extreme Q rates.

The wide oscillation between dry and wet extremes is expected to cause strong perturbations that hamper the adaptive capacity of riverine and marine [82] species. In dry years, nitrate and soluble reactive phosphorus attain very low loadings in summer, when the

physical conditions of coastal and marine waters are optimal for primary production [83]. The drought phase is thus expected to trigger a sort of mismatch between nutrient availability and marine primary productivity, with cascade effects in marine food webs. In contrast, the maximum loads estimated in very wet years could again stimulate eutrophication. The agricultural sector is known to directly increase nutrient loads with fertilisers and manure application, also depending on irrigation techniques and water availability [105–107]. Our results suggest that the interaction between the hydrological variability induced by climate change and direct anthropic water consumption can influence the interannual variation in N and P loads. This is a critical point that refers to the N and P legacy and its delayed release to aquatic environments.

**Supplementary Materials:** The following supporting information can be downloaded at: <https://www.mdpi.com/article/10.3390/w16182628/s1>; Figure S1: Land use distribution in the study area (Corine Land Cover (2018)); Figure S2: Altitude distribution (m a.s.l) in the study area; Figure S3: Relationship between water discharges ( $\text{m}^3 \text{s}^{-1}$ ) measured at Ficarolo station versus Pontelagoscuro station, with data from 1992 to 2022; Figure S4: Log-log relationship between water discharge versus precipitation. Coloured line represents a significant relationship ( $p < 0.05$ ); Figure S5: Log-log relationship between nutrient loads versus precipitation with annual data. Figure S6: Log-log relationship between loads versus precipitation. Coloured line represents significant relationship ( $p < 0.05$ ); Figure S7: log-log relationship between concentration versus water discharge with whole dataset; Figure S8: log-log relationship between concentration versus water discharge. Coloured line represents a significant relationship ( $p < 0.05$ ); Table S1: Log-log relationship between water discharge versus precipitation.  $p$ -values refer to slope; Table S2: Log-log relationship between loads versus precipitation.  $p$ -values refer to slope; Table S3: Log-log relationship between concentration versus water discharge.  $p$ -values refer to slope. Table S4: Log-log relationship between concentration versus water discharge.  $p$ -values refer to slope.

**Author Contributions:** Conceptualisation: E.C., P.V. and D.N.; data collection and analysis: E.C., S.F., A.S. and E.B.; writing—original draft preparation: E.C., P.V.; writing—review and editing: D.N., M.N., M.S., A.S., E.B. and S.F. All authors have read and agreed to the published version of the manuscript.

**Funding:** This research is part of a Scientific Agreement between the Universities of Parma, Ferrara and Turin and the River Po Basin District Authority (Origin and dynamics of nutrient loads from the River Po basin and other basins flowing into the Adriatic Sea) funded by the Italian Development and Cohesion Fund of the Ministry of the Environment and Energy Security. E.C was supported by the Cariparma Foundation through a PhD fellowship.

**Data Availability Statement:** No public dataset was created for this study. Upon request, we are available to provide any data.

**Acknowledgments:** This study is part of a PhD project by Edoardo Cavallini, PhD course in Evolutionary Biology and Ecology, cycle 36. We acknowledge ARPAE Emilia-Romagna for providing water quality data and River Po Authority for supporting this study. We are especially indebted to Fernanda Moroni for all the help and support provided during the research.

**Conflicts of Interest:** The authors declare no conflicts of interest. The funders had no role in the design of the study; in the collection, analyses, or interpretation of data; in the writing of the manuscript; or in the decision to publish the results.

## References

1. Lheureux, A.; David, V.; Del Amo, Y.; Soudant, D.; Auby, I.; Bozec, Y.; Conan, P.; Ganthy, F.; Grégori, G.; Lefebvre, A.; et al. Trajectories of Nutrients Concentrations and Ratios in the French Coastal Ecosystems: 20 Years of Changes in Relation with Large-Scale and Local Drivers. *Sci. Total Environ.* **2023**, *857*, 159619. [[CrossRef](#)] [[PubMed](#)]
2. Romero, E.; Garnier, J.; Lassaletta, L.; Billen, G.; Le Gendre, R.; Riou, P.; Cugier, P. Large-Scale Patterns of River Inputs in South-western Europe: Seasonal and Interannual Variations and Potential Eutrophication Effects at the Coastal Zone. *Biogeochemistry* **2013**, *113*, 481–505. [[CrossRef](#)]
3. Smith, V.H.; Schindler, D.W. Eutrophication Science: Where Do We Go from Here? *Trends Ecol. Evol.* **2009**, *24*, 201–207. [[CrossRef](#)]
4. Van Meter, K.J.; Chowdhury, S.; Byrnes, D.K.; Basu, N.B. Biogeochemical Asynchrony: Ecosystem Drivers of Seasonal Concentration Regimes across the Great Lakes Basin. *Limnol. Oceanogr.* **2020**, *65*, 848–862. [[CrossRef](#)]



5. Grizzetti, B.; Bouraoui, F.; Aloe, A. Changes of Nitrogen and Phosphorus Loads to European Seas. *Glob. Change Biol.* **2012**, *18*, 769–782. [[CrossRef](#)]
6. Hilton, J.; O'Hare, M.; Bowes, M.J.; Jones, J.I. How Green Is My River? A New Paradigm of Eutrophication in Rivers. *Sci. Total Environ.* **2006**, *365*, 66–83. [[CrossRef](#)]
7. Le Moal, M.; Gascuel-Oudou, C.; Ménesguen, A.; Souchon, Y.; Étrillard, C.; Levain, A.; Moatar, F.; Pannard, A.; Souchu, P.; Lefebvre, A.; et al. Eutrophication: A New Wine in an Old Bottle? *Sci. Total Environ.* **2019**, *651*, 1–11. [[CrossRef](#)]
8. Smith, V.H.; Tilman, G.D.; Nekola, J.C. Eutrophication: Impacts of Excess Nutrient Inputs on Freshwater, Marine, and Terrestrial Ecosystems. *Environ. Pollut.* **1999**, *100*, 179–196. [[CrossRef](#)]
9. Goyette, J.O.; Bennett, E.M.; Maranger, R. Differential Influence of Landscape Features and Climate on Nitrogen and Phosphorus Transport throughout the Watershed. *Biogeochemistry* **2019**, *142*, 155–174. [[CrossRef](#)]
10. Howarth, R.; Swaney, D.; Billen, G.; Garnier, J.; Hong, B.; Humborg, C.; Johnes, P.; Mörth, C.M.; Marino, R. Nitrogen Fluxes from the Landscape Are Controlled by Net Anthropogenic Nitrogen Inputs and by Climate. *Front. Ecol. Environ.* **2012**, *10*, 37–43. [[CrossRef](#)]
11. Lassaletta, L.; Romero, E.; Billen, G.; Garnier, J.; García-Gómez, H.; Rovira, J.V. Spatialized N Budgets in a Large Agricultural Mediterranean Watershed: High Loading and Low Transfer. *Biogeosciences* **2012**, *9*, 57–70. [[CrossRef](#)]
12. Viaroli, P.; Soana, E.; Pecora, S.; Laini, A.; Naldi, M.; Fano, E.A.; Nizzoli, D. Space and Time Variations of Watershed N and P Budgets and Their Relationships with Reactive N and P Loadings in a Heavily Impacted River Basin (Po River, Northern Italy). *Sci. Total Environ.* **2018**, *639*, 1574–1587. [[CrossRef](#)] [[PubMed](#)]
13. Glibert, P.M. Eutrophication, Harmful Algae and Biodiversity—Challenging Paradigms in a World of Complex Nutrient Changes. *Mar. Pollut. Bull.* **2017**, *124*, 591–606. [[CrossRef](#)]
14. Houser, J.N.; Richardson, W.B. Nitrogen and Phosphorus in the Upper Mississippi River: Transport, Processing, and Effects on the River Ecosystem. *Hydrobiologia* **2010**, *640*, 71–88. [[CrossRef](#)]
15. Jarvie, H.P.; Pallett, D.W.; Schäfer, S.M.; Macrae, M.L.; Bowes, M.J.; Farrand, P.; Warwick, A.C.; King, S.M.; Williams, R.J.; Armstrong, L.; et al. Biogeochemical and Climate Drivers of Wetland Phosphorus and Nitrogen Release: Implications for Nutrient Legacies and Eutrophication Risk. *J. Environ. Qual.* **2020**, *49*, 1703–1716. [[CrossRef](#)] [[PubMed](#)]
16. Racchetti, E.; Bartoli, M.; Soana, E.; Longhi, D.; Christian, R.R.; Pinaridi, M.; Viaroli, P. Influence of Hydrological Connectivity of Riverine Wetlands on Nitrogen Removal via Denitrification. *Biogeochemistry* **2011**, *103*, 335–354. [[CrossRef](#)]
17. Wolf, K.L.; Noe, G.B.; Ahn, C. Hydrologic Connectivity to Streams Increases Nitrogen and Phosphorus Inputs and Cycling in Soils of Created and Natural Floodplain Wetlands. *J. Environ. Qual.* **2013**, *42*, 1245–1255. [[CrossRef](#)]
18. Tockner, K.; Malard, F.; Ward, J.V. An Extension of the Flood Pulse Concept. *Hydrol. Process.* **2000**, *14*, 2861–2883. [[CrossRef](#)]
19. Hirabayashi, Y.; Kanae, S.; Emori, S.; Oki, T.; Kimoto, M. Global Projections of Changing Risks of Floods and Droughts in a Changing Climate. *Hydrol. Sci. J.* **2008**, *53*, 754–772. [[CrossRef](#)]
20. Kundzewicz, Z.W.; Pin'skwar, I.; Brakenridge, G.R. Changes in River Flood Hazard in Europe: A Review. *Hydrol. Res.* **2018**, *49*, 294–302. [[CrossRef](#)]
21. Kunkel, K.E.; Easterling, D.R.; Redmond, K.; Hubbard, K. Temporal Variations of Extreme Precipitation Events in the United States: 1895–2000. *Geophys. Res. Lett.* **2003**, *30*, 1895–2000. [[CrossRef](#)]
22. Satoh, Y.; Yoshimura, K.; Pokhrel, Y.; Kim, H.; Shiogama, H.; Yokohata, T.; Hanasaki, N.; Wada, Y.; Burek, P.; Byers, E.; et al. The Timing of Unprecedented Hydrological Drought under Climate Change. *Nat. Commun.* **2022**, *13*, 3287. [[CrossRef](#)] [[PubMed](#)]
23. Attygalla, N.W.; Baldwin, D.S.; Silvester, E.; Kappen, P.; Whitworth, K.L. The Severity of Sediment Desiccation Affects the Adsorption Characteristics and Speciation of Phosphorus. *Environ. Sci. Process. Impacts* **2016**, *18*, 64–71. [[CrossRef](#)] [[PubMed](#)]
24. Homyak, P.M.; Allison, S.D.; Huxman, T.E.; Goulden, M.L.; Treseder, K.K. Effects of Drought Manipulation on Soil Nitrogen Cycling: A Meta-Analysis. *J. Geophys. Res. Biogeosci.* **2017**, *122*, 3260–3272. [[CrossRef](#)]
25. Merbt, S.N.; Proia, L.; Prosser, J.I.; Marti, E.; Casamayor, E.O.; Von Schiller, D. Stream Drying Drives Microbial Ammonia Oxidation and First-Flush Nitrate Export. *Ecology* **2016**, *97*, 2192–2198. [[CrossRef](#)] [[PubMed](#)]
26. Ramos, M.C.; Lizaga, I.; Gaspar, L.; Quijano, L.; Navas, A. Effects of Rainfall Intensity and Slope on Sediment, Nitrogen and Phosphorus Losses in Soils with Different Use and Soil Hydrological Properties. *Agric. Water Manag.* **2019**, *226*, 105789. [[CrossRef](#)]
27. Lucas, E.; Kennedy, B.; Roswall, T.; Burgis, C.; Toor, G.S. Climate Change Effects on Phosphorus Loss from Agricultural Land to Water: A Review. *Curr. Pollut. Rep.* **2023**, *9*, 623–645. [[CrossRef](#)]
28. Kreiling, R.M.; Richardson, W.B.; Bartsch, L.A.; Thoms, M.C.; Christensen, V.G. Denitrification in the River Network of a Mixed Land Use Watershed: Unpacking the Complexities. *Biogeochemistry* **2019**, *143*, 327–346. [[CrossRef](#)]
29. Shrestha, J.; Niklaus, P.A.; Pasquale, N.; Huber, B.; Barnard, R.L.; Frossard, E.; Schleppei, P.; Tockner, K.; Luster, J. Flood Pulses Control Soil Nitrogen Cycling in a Dynamic River Floodplain. *Geoderma* **2014**, *228–229*, 14–24. [[CrossRef](#)]
30. Jarvie, H.P.; Sharpley, A.N.; Withers, P.J.A.; Scott, J.T.; Haggard, B.E.; Neal, C. Phosphorus Mitigation to Control River Eutrophication: Murky Waters, Inconvenient Truths, and “Postnormal” Science. *J. Environ. Qual.* **2013**, *42*, 295–304. [[CrossRef](#)]
31. Withers, P.J.A.; Jarvie, H.P. Delivery and Cycling of Phosphorus in Rivers: A Review. *Sci. Total Environ.* **2008**, *400*, 379–395. [[CrossRef](#)] [[PubMed](#)]
32. Abbott, B.W.; Moatar, F.; Gauthier, O.; Fovet, O.; Antoine, V.; Ragueneau, O. Trends and Seasonality of River Nutrients in Agricultural Catchments: 18 Years of Weekly Citizen Science in France. *Sci. Total Environ.* **2018**, *624*, 845–858. [[CrossRef](#)] [[PubMed](#)]

33. Ebeling, P.; Dupas, R.; Abbott, B.; Kumar, R.; Ehrhardt, S.; Fleckenstein, J.H.; Musolff, A. Long-Term Nitrate Trajectories Vary by Season in Western European Catchments. *Glob. Biogeochem. Cycles* **2021**, *35*, e2021GB007050. [[CrossRef](#)]
34. Carrer, M.; Dibona, R.; Prendin, A.L.; Brunetti, M. Recent Waning Snowpack in the Alps Is Unprecedented in the Last Six Centuries. *Nat. Clim. Change* **2023**, *13*, 155–160. [[CrossRef](#)]
35. Chiarle, M.; Geertsema, M.; Mortara, G.; Clague, J.J. Relations between Climate Change and Mass Movement: Perspectives from the Canadian Cordillera and the European Alps. *Glob. Planet. Change* **2021**, *202*, 103499. [[CrossRef](#)]
36. Lionello, P.; Scarascia, L. The Relation between Climate Change in the Mediterranean Region and Global Warming. *Reg. Environ. Change* **2018**, *18*, 1481–1493. [[CrossRef](#)]
37. Heathwaite, L.; Haygarth, P.; Matthews, R.; Preedy, N.; Butler, P. Evaluating Colloidal Phosphorus Delivery to Surface Waters from Diffuse Agricultural Sources. *J. Environ. Qual.* **2005**, *34*, 287–298. [[CrossRef](#)]
38. Howarth, R.W.; Marino, R. Nitrogen as the Limiting Nutrient for Eutrophication in Coastal Marine Ecosystems: Evolving Views over Three Decades. *Limnol. Oceanogr.* **2006**, *51*, 364–376. [[CrossRef](#)]
39. Ockenden, M.C.; Deasy, C.E.; Benskin, C.M.W.H.; Beven, K.J.; Burke, S.; Collins, A.L.; Evans, R.; Falloon, P.D.; Forber, K.J.; Hiscock, K.M.; et al. Changing Climate and Nutrient Transfers: Evidence from High Temporal Resolution Concentration-Flow Dynamics in Headwater Catchments. *Sci. Total Environ.* **2016**, *548–549*, 325–339. [[CrossRef](#)]
40. Galloway, N.J. The Global Nitrogen Cycle. *TrGeo* **2003**, *8*, 682. [[CrossRef](#)]
41. Matiatos, I.; Wassenaar, L.I.; Monteiro, L.R.; Venkiteswaran, J.J.; Gooddy, D.C.; Boeckx, P.; Sacchi, E.; Yue, F.J.; Michalski, G.; Alonso-Hernández, C.; et al. Global Patterns of Nitrate Isotope Composition in Rivers and Adjacent Aquifers Reveal Reactive Nitrogen Cascading. *Commun. Earth Environ.* **2021**, *2*, 52. [[CrossRef](#)]
42. Kincaid, D.W.; Seybold, E.C.; Adair, E.C.; Bowden, W.B.; Perdrial, J.N.; Vaughan, M.C.H.; Schroth, A.W. Land Use and Season Influence Event-Scale Nitrate and Soluble Reactive Phosphorus Exports and Export Stoichiometry from Headwater Catchments. *Water Resour. Res.* **2020**, *56*, e2020WR027361. [[CrossRef](#)]
43. Shousha, S.; Maranger, R.; Lapierre, J.F. Different Forms of Carbon, Nitrogen, and Phosphorus Influence Ecosystem Stoichiometry in a North Temperate River across Seasons and Land Uses. *Limnol. Oceanogr.* **2021**, *66*, 4285–4298. [[CrossRef](#)]
44. Strohmenger, L.; Fovet, O.; Akkal-Corfini, N.; Dupas, R.; Durand, P.; Faucheux, M.; Gruau, G.; Hamon, Y.; Jaffrezic, A.; Minaudo, C.; et al. Multitemporal Relationships Between the Hydroclimate and Exports of Carbon, Nitrogen, and Phosphorus in a Small Agricultural Watershed. *Water Resour. Res.* **2020**, *56*, e2019WR026323. [[CrossRef](#)]
45. Qiu, J.; Shen, Z.; Leng, G.; Wei, G. Synergistic Effect of Drought and Rainfall Events of Different Patterns on Watershed Systems. *Sci. Rep.* **2021**, *11*, 18957. [[CrossRef](#)]
46. Seybold, E.C.; Dwivedi, R.; Musselman, K.N.; Kincaid, D.W.; Schroth, A.W.; Classen, A.T.; Perdrial, J.N.; Adair, E.C. Winter Runoff Events Pose an Unquantified Continental-Scale Risk of High Wintertime Nutrient Export. *Environ. Res. Lett.* **2022**, *17*, 104044. [[CrossRef](#)]
47. Karimi, K.; Miller, J.W.; Sankarasubramanian, A.; Obenour, D.R. Contrasting Annual and Summer Phosphorus Export Using a Hybrid Bayesian Watershed Model. *Water Resour. Res.* **2023**, *59*, e2022WR033088. [[CrossRef](#)]
48. Skoulikidis, N.T.; Sabater, S.; Detry, T.; Morais, M.M.; Buffagni, A.; Dörflinger, G.; Zogaris, S.; del Mar Sánchez-Montoya, M.; Bonada, N.; Kalogianni, E.; et al. Non-Perennial Mediterranean Rivers in Europe: Status, Pressures, and Challenges for Research and Management. *Sci. Total Environ.* **2017**, *577*, 1–18. [[CrossRef](#)]
49. Costa, D.; Sutter, C.; Shepherd, A.; Jarvie, H.; Wilson, H.; Elliott, J.; Liu, J.; Macrae, M. Impact of Climate Change on Catchment Nutrient Dynamics: Insights from around the World. *Environ. Rev.* **2022**, *31*, 4–25. [[CrossRef](#)]
50. Speir, S.L.; Rose, L.A.; Blaszczyk, J.R.; Kincaid, D.W.; Fazekas, H.M.; Webster, A.J.; Wolford, M.A.; Shogren, A.J.; Wymore, A.S. Catchment Concentration–Discharge Relationships across Temporal Scales: A Review. *Wiley Interdiscip. Rev. Water* **2024**, *11*, e1702. [[CrossRef](#)]
51. Montanari, A.; Nguyen, H.; Rubinetti, S.; Ceola, S.; Galelli, S.; Rubino, A.; Zanchettin, D. Why the 2022 Po River Drought Is the Worst in the Past Two Centuries. *Sci. Adv.* **2023**, *9*, eadg8304. [[CrossRef](#)] [[PubMed](#)]
52. Polade, S.D.; Gershunov, A.; Cayan, D.R.; Dettinger, M.D.; Pierce, D.W. Precipitation in a Warming World: Assessing Projected Hydro-Climate Changes in California and Other Mediterranean Climate Regions. *Sci. Rep.* **2017**, *7*, 10783. [[CrossRef](#)] [[PubMed](#)]
53. Colombo, N.; Valt, M.; Romano, E.; Salerno, F.; Godone, D.; Cianfarra, P.; Freppaz, M.; Maugeri, M.; Guyennon, N. Long-Term Trend of Snow Water Equivalent in the Italian Alps. *J. Hydrol.* **2022**, *614*, 128532. [[CrossRef](#)]
54. Piano, E.; Doretto, A.; Falasco, E.; Gruppuso, L.; Fenoglio, S.; Bona, F. The Role of Recurrent Dewatering Events in Shaping Ecological Niches of Scrapers in Intermittent Alpine Streams. *Hydrobiologia* **2019**, *841*, 177–189. [[CrossRef](#)]
55. Marchetti, R.; Provini, A.; Crosa, G. Nutrient Load Carried by the River Po into the Adriatic Sea, 1968–1987. *Mar. Pollut. Bull.* **1989**, *20*, 168–172. [[CrossRef](#)]
56. Cozzi, S.; Ibáñez, C.; Lazar, L.; Raimbault, P.; Giani, M. Flow Regime and Nutrient-Loading Trends from the Largest South European Watersheds: Implications for the Productivity of Mediterranean and Black Sea’s Coastal Areas. *Water* **2018**, *11*, 1. [[CrossRef](#)]
57. Cozzi, S.; Giani, M. River Water and Nutrient Discharges in the Northern Adriatic Sea: Current Importance and Long Term Changes. *Cont. Shelf Res.* **2011**, *31*, 1881–1893. [[CrossRef](#)]

58. Soana, E.; Gervasio, M.P.; Granata, T.; Colombo, D.; Castaldelli, G. Climate Change Impacts on Eutrophication in the Po River (Italy): Temperature-Mediated Reduction in Nitrogen Export but No Effect on Phosphorus. *J. Environ. Sci.* **2024**, *143*, 148–163. [CrossRef]
59. Bierozza, M.Z.; Heathwaite, A.L.; Bechmann, M.; Kyllmar, K.; Jordan, P. The Concentration-Discharge Slope as a Tool for Water Quality Management. *Sci. Total Environ.* **2018**, *630*, 738–749. [CrossRef]
60. Moatar, F.; Abbott, B.W.; Minaudo, C.; Curie, F.; Pinay, G. Elemental Properties, Hydrology, and Biology Interact to Shape Concentration-Discharge Curves for Carbon, Nutrients, Sediment, and Major Ions. *Water Resour. Res.* **2017**, *53*, 1270–1287. [CrossRef]
61. Musolff, A.; Schmidt, C.; Selle, B.; Fleckenstein, J.H. Catchment Controls on Solute Export. *Adv. Water Resour.* **2015**, *86*, 133–146. [CrossRef]
62. Ludwig, W.; Bouwman, A.F.; Dumont, E.; Lespinas, F. Water and Nutrient Fluxes from Major Mediterranean and Black Sea Rivers: Past and Future Trends and Their Implications for the Basin-Scale Budgets. *Glob. Biogeochem. Cycles* **2010**, *24*, 13. [CrossRef]
63. Viaroli, P.; Puma, F.; Ferrari, I. Aggiornamento Delle Conoscenze Ecologiche Sul Bacino Idrografico Padano: Una Sintesi. *Biol. Ambient.* **2010**, *24*, 7–19.
64. Autorità di Bacino del fiume Po Piano Del Bilancio Idrico per Il Distretto Del Fiume Po. Parma, Italy. 2016. Available online: <https://pianobilancioidrico.adbpo.it/progetto-di-piano-di-bilancio-idrico/> (accessed on 15 January 2024).
65. Turco, M.; Vezzoli, R.; Da Ronco, P.; Mercogliano, P. Variation in Discharge, Precipitation and Temperature in Po River and Tributaries Basins. *CMCC Research Paper* **2013**, 185. [CrossRef]
66. Montanari, A. Hydrology of the Po River: Looking for Changing Patterns in River Discharge. *Hydrol. Earth Syst. Sci.* **2012**, *16*, 3739–3747. [CrossRef]
67. APAT-IRSA/CNR. *Metodi Analitici per Le Acque*; Manuali e Linee Guida; APAT: Roma, Italy, 2003; Volume 29, ISBN 88-448-0083-7.
68. Cornes, R.C.; van der Schrier, G.; van den Besselaar, E.J.M.; Jones, P.D. An Ensemble Version of the E-OBS Temperature and Precipitation Data Sets. *J. Geophys. Res. Atmos.* **2018**, *123*, 9391–9409. [CrossRef]
69. Quilbé, R.; Rousseau, A.N.; Duchemin, M.; Poulin, A.; Gangbazo, G.; Villeneuve, J.P. Selecting a Calculation Method to Estimate Sediment and Nutrient Loads in Streams: Application to the Beaurivage River (Québec, Canada). *J. Hydrol.* **2006**, *326*, 295–310. [CrossRef]
70. Thompson, S.E.; Basu, N.B.; Lascurain, J.; Aubeneau, A.; Rao, P.S.C. Relative Dominance of Hydrologic versus Biogeochemical Factors on Solute Export across Impact Gradients. *Water Resour. Res.* **2011**, *47*. [CrossRef]
71. Godsey, S.E.; Kirchner, J.W.; Clow, D.W. Concentration-Discharge Relationships Reflect Chemostatic Characteristics of US Catchments. *Hydrol. Process.* **2009**, *23*, 1844–1864. [CrossRef]
72. R Core Team. *R: A Language and Environment for Statistical Computing*; R Foundation for Statistical Computing: Vienna, Austria, 2022.
73. Wood, S.N. *Generalized Additive Models: An Introduction with R*, 2nd ed.; Chapman and Hall/CRC: New York, NY, USA, 2017. [CrossRef]
74. Pedersen, E.J.; Miller, D.L.; Simpson, G.L.; Ross, N. Hierarchical Generalized Additive Models in Ecology: An Introduction with Mgc. *PeerJ* **2019**, *7*, e6876. [CrossRef]
75. Zuur, A.F.; Ieno, E.N.; Walker, N.; Saveliev, A.A.; Smith, G.M. *Mixed Effects Models and Extensions in Ecology with R*; Springer: New York, NY, USA, 2009. [CrossRef]
76. Wachholz, A.; Jawitz, J.W.; Büttner, O.; Jomaa, S.; Merz, R.; Yang, S.; Borchardt, D. Drivers of Multi-Decadal Nitrate Regime Shifts in a Large European Catchment. *Environ. Res. Lett.* **2022**, *17*, 064039. [CrossRef]
77. Zoboli, O.; Viglione, A.; Rechberger, H.; Zessner, M. Impact of Reduced Anthropogenic Emissions and Century Flood on the Phosphorus Stock, Concentrations and Loads in the Upper Danube. *Sci. Total Environ.* **2015**, *518–519*, 117–129. [CrossRef] [PubMed]
78. McCrackin, M.L.; Muller-Karulis, B.; Gustafsson, B.G.; Howarth, R.W.; Humborg, C.; Svanbäck, A.; Swaney, D.P. A Century of Legacy Phosphorus Dynamics in a Large Drainage Basin. *Glob. Biogeochem. Cycles* **2018**, *32*, 1107–1122. [CrossRef]
79. Zanchettin, D.; Traverso, P.; Tomasino, M. Po River Discharges: A Preliminary Analysis of a 200-Year Time Series. *Clim. Change* **2008**, *89*, 411–433. [CrossRef]
80. Djakovac, T.; Degobbi, D.; Supić, N.; Precali, R. Marked Reduction of Eutrophication Pressure in the Northeastern Adriatic in the Period 2000–2009. *Estuar. Coast. Shelf Sci.* **2012**, *115*, 25–32. [CrossRef]
81. Giani, M.; Djakovac, T.; Degobbi, D.; Cozzi, S.; Solidoro, C.; Umani, S.F. Recent Changes in the Marine Ecosystems of the Northern Adriatic Sea. *Estuar. Coast. Shelf Sci.* **2012**, *115*, 1–13. [CrossRef]
82. Marini, M.; Grilli, F. The Role of Nitrogen and Phosphorus in Eutrophication of the Northern Adriatic Sea: History and Future Scenarios. *Appl. Sci.* **2023**, *13*, 9267. [CrossRef]
83. Neri, F.; Romagnoli, T.; Accoroni, S.; Campanelli, A.; Marini, M.; Grilli, F.; Totti, C. Phytoplankton and Environmental Drivers at a Long-Term Offshore Station in the Northern Adriatic Sea (1988–2018). *Cont. Shelf Res.* **2022**, *242*, 104746. [CrossRef]
84. Grilli, F.; Accoroni, S.; Acri, F.; Aubry, F.B.; Bergami, C.; Cabrini, M.; Campanelli, A.; Giani, M.; Guicciardi, S.; Marini, M.; et al. Seasonal and Interannual Trends of Oceanographic Parameters over 40 Years in the Northern Adriatic Sea in Relation to Nutrient Loadings Using the EMODnet Chemistry Data Portal. *Water* **2020**, *12*, 2280. [CrossRef]

85. Holmes, R.M.; McClelland, J.W.; Peterson, B.J.; Tank, S.E.; Bulygina, E.; Eglinton, T.I.; Gordeev, V.V.; Gurtovaya, T.Y.; Raymond, P.A.; Repeta, D.J.; et al. Seasonal and Annual Fluxes of Nutrients and Organic Matter from Large Rivers to the Arctic Ocean and Surrounding Seas. *Estuaries Coasts* **2012**, *35*, 369–382. [[CrossRef](#)]
86. Thomas, Z.; Abbott, B.W.; Troccaz, O.; Baudry, J.; Pinay, G. Proximate and Ultimate Controls on Carbon and Nutrient Dynamics of Small Agricultural Catchments. *Biogeosciences* **2016**, *13*, 1863–1875. [[CrossRef](#)]
87. Romero, E.; Ludwig, W.; Sadaoui, M.; Lassaletta, L.; Bouwman, A.F.; Beusen, A.H.W.; van Apeldoorn, D.; Sardans, J.; Janssens, I.A.; Ciais, P.; et al. The Mediterranean Region as a Paradigm of the Global Decoupling of N and P Between Soils and Freshwaters. *Glob. Biogeochem. Cycles* **2021**, *35*, e2020GB006874. [[CrossRef](#)]
88. Bauwe, A.; Kahle, P.; Tiemeyer, B.; Lennartz, B. Hydrology Is the Key Factor for Nitrogen Export from Tile-Drained Catchments under Consistent Land-Management. *Environ. Res. Lett.* **2020**, *15*, 094050. [[CrossRef](#)]
89. Cuadra, P.E.; Vidon, P. Storm Nitrogen Dynamics in Tile-Drain Flow in the US Midwest. *Biogeochemistry* **2011**, *104*, 293–308. [[CrossRef](#)]
90. Speir, S.L.; Tank, J.L.; Bierzoza, M.; Mahl, U.H.; Royer, T.V. Storm Size and Hydrologic Modification Influence Nitrate Mobilization and Transport in Agricultural Watersheds. *Biogeochemistry* **2021**, *156*, 319–334. [[CrossRef](#)]
91. Bernhardt, E.S.; Heffernan, J.B.; Grimm, N.B.; Stanley, E.H.; Harvey, J.W.; Arroita, M.; Appling, A.P.; Cohen, M.J.; McDowell, W.H.; Hall, R.O.; et al. The Metabolic Regimes of Flowing Waters. *Limnol. Oceanogr.* **2018**, *63*, S99–S118. [[CrossRef](#)]
92. Tavernini, S.; Pierobon, E.; Viaroli, P. Physical Factors and Dissolved Reactive Silica Affect Phytoplankton Community Structure and Dynamics in a Lowland Eutrophic River (Po River, Italy). *Hydrobiologia* **2011**, *669*, 213–225. [[CrossRef](#)]
93. Outram, F.N.; Cooper, R.J.; Sünnerberg, G.; Hiscock, K.M.; Lovett, A.A. Antecedent Conditions, Hydrological Connectivity and Anthropogenic Inputs: Factors Affecting Nitrate and Phosphorus Transfers to Agricultural Headwater Streams. *Sci. Total Environ.* **2016**, *545–546*, 184–199. [[CrossRef](#)]
94. Zimmer, M.A.; Pellerin, B.; Burns, D.A.; Petrochenkov, G. Temporal Variability in Nitrate-Discharge Relationships in Large Rivers as Revealed by High-Frequency Data. *Water Resour. Res.* **2019**, *55*, 973–989. [[CrossRef](#)]
95. Schulz, G.; van Beusekom, J.E.E.; Jacob, J.; Bold, S.; Schöl, A.; Ankele, M.; Sanders, T.; Dähnke, K. Low Discharge Intensifies Nitrogen Retention in Rivers—A Case Study in the Elbe River. *Sci. Total Environ.* **2023**, *904*, 166740. [[CrossRef](#)]
96. Bierzoza, M.Z.; Heathwaite, A.L. Seasonal Variation in Phosphorus Concentration–Discharge Hysteresis Inferred from High-Frequency in Situ Monitoring. *J. Hydrol.* **2015**, *524*, 333–347. [[CrossRef](#)]
97. Dolph, C.L.; Boardman, E.; Danesh-Yazdi, M.; Finlay, J.C.; Hansen, A.T.; Baker, A.C.; Dalzell, B. Phosphorus Transport in Intensively Managed Watersheds. *Water Resour. Res.* **2019**, *55*, 9148–9172. [[CrossRef](#)]
98. Tesi, T.; Miserocchi, S.; Aciri, F.; Langone, L.; Boldrin, A.; Hatten, J.A.; Albertazzi, S. Flood-Driven Transport of Sediment, Particulate Organic Matter, and Nutrients from the Po River Watershed to the Mediterranean Sea. *J. Hydrol.* **2013**, *498*, 144–152. [[CrossRef](#)]
99. Pilotti, M.; Barone, L.; Balistocchi, M.; Valerio, G.; Milanese, L.; Nizzoli, D. Nutrient Delivery Efficiency of a Combined Sewer along a Lake Challenged by Incipient Eutrophication. *Water Res.* **2021**, *190*, 116727. [[CrossRef](#)]
100. Minaudo, C.; Dupas, R.; Gascuel-Oudou, C.; Roubeix, V.; Danis, P.A.; Moatar, F. Seasonal and Event-Based Concentration-Discharge Relationships to Identify Catchment Controls on Nutrient Export Regimes. *Adv. Water Resour.* **2019**, *131*, 103379. [[CrossRef](#)]
101. Ebeling, P.; Kumar, R.; Weber, M.; Knoll, L.; Fleckenstein, J.H.; Musolff, A. Archetypes and Controls of Riverine Nutrient Export Across German Catchments. *Water Resour. Res.* **2021**, *57*, e2020WR028134. [[CrossRef](#)]
102. Basu, N.B.; Thompson, S.E.; Rao, P.S.C. Hydrologic and Biogeochemical Functioning of Intensively Managed Catchments: A Synthesis of Top-down Analyses. *Water Resour. Res.* **2011**, *47*, e2011WR010800. [[CrossRef](#)]
103. Musolff, A.; Schmidt, C.; Rode, M.; Lischeid, G.; Weise, S.M.; Fleckenstein, J.H. Groundwater Head Controls Nitrate Export from an Agricultural Lowland Catchment. *Adv. Water Resour.* **2016**, *96*, 95–107. [[CrossRef](#)]
104. Winter, C.; Lutz, S.R.; Musolff, A.; Kumar, R.; Weber, M.; Fleckenstein, J.H. Disentangling the Impact of Catchment Heterogeneity on Nitrate Export Dynamics From Event to Long-Term Time Scales. *Water Resour. Res.* **2021**, *57*, e2020WR027992. [[CrossRef](#)]
105. Casquin, A.; Dupas, R.; Gu, S.; Couic, E.; Gruau, G.; Durand, P. The Influence of Landscape Spatial Configuration on Nitrogen and Phosphorus Exports in Agricultural Catchments. *Landsc. Ecol.* **2021**, *36*, 3383–3399. [[CrossRef](#)]
106. Lassaletta, L.; Sanz-Cobena, A.; Aguilera, E.; Quemada, M.; Billen, G.; Bondeau, A.; Cayuela, M.L.; Cramer, W.; Eekhout, J.P.C.; Garnier, J.; et al. Nitrogen Dynamics in Cropping Systems under Mediterranean Climate: A Systemic Analysis. *Environ. Res. Lett.* **2021**, *16*, 073002. [[CrossRef](#)]
107. Metre, P.C.V.; Frey, J.W.; Musgrove, M.; Nakagaki, N.; Qi, S.; Mahler, B.J.; Wiczorek, M.E.; Button, D.T. High Nitrate Concentrations in Some Midwest United States Streams in 2013 after the 2012 Drought. *J. Environ. Qual.* **2016**, *45*, 1696–1704. [[CrossRef](#)] [[PubMed](#)]

**Disclaimer/Publisher’s Note:** The statements, opinions and data contained in all publications are solely those of the individual author(s) and contributor(s) and not of MDPI and/or the editor(s). MDPI and/or the editor(s) disclaim responsibility for any injury to people or property resulting from any ideas, methods, instructions or products referred to in the content.